From June 2010 *High Frequency Electronics*

An Analytic and Graphical Method for LNA Design with Feedback

By Alan Victor, Nitronex Corp., and Jayesh Nath, Aviat Networks

This article explores the trade-offs between gain, match and noise figure in a low noise amplifier, resulting in a new figure-of-merit for selecting the value of source inductance

An analytic technique and figure-of-merit (F_{nm}) for the trade-off of noise measure and mismatch loss in the design of low noise amplifier is presented. The trade-off between various design parameters as a function of inductive source degeneration is evaluated using the developed design curve. It is shown that the design curves are unique to the selected device. Several devices demonstrated conditions whereby the use of source degeneration leads to instability and must be avoided. The technique is straightforward and permits prescreening of potential devices being considered for low noise amplifier design. The resulting design curves permit accurate selection of the range of acceptable feedback values to achieve desired performance. A new figure-of-merit has been introduced which allows designers to choose the optimum value of source inductance either analytically or graphically. The new methodology is discussed and was applied to low noise pseudomorphic hetero-junction FET (pH-JFET) amplifier designs at 2.10 GHz and 10.24 GHz.

I. An Overview of Design Techniques

Noise figure, available gain, and return loss or the port VSWR are key elements in low noise amplifier design. Low noise figure without adequate gain or poor return loss degrades system performance. High gain without adequate noise figure also compromises system performance. Optimizing the input noise figure of an active stage, irrespective of the impedance presented to the source, preserves the noise figure, however at the expense of other parametric values. For example, high port VSWR can lead to excessive passband insertion loss when filters are used, as in a preselector design, or can results in excessive group delay distortion. Consequently, although the noise figure may be excellent, the system performance can suffer significantly. System performance is degraded due to an increase in inter-symbol interference and lack of decoding sensitivity.

Noise measure [2] was introduced as a figure-of-merit tying together two key components in amplifier design, noise figure and gain. The noise measure M is defined as:

$$M = (F - 1)/(1 - 1/G_a) \quad (1)$$

Where F is the noise factor (numeric noise figure) and G_a is the numeric amplifier available gain.

The goal is to minimize the noise measure, that is achieve as low a noise figure as possible while maximizing the amplifier available gain. The desired result is to minimize second stage noise contribution in a cascaded system. In addition, although not part of noise measure, this should be achieved with a low port VSWR. Mismatch loss and excessive input VSWR for an individual amplifier noise figure is not an issue. A necessarily high input VSWR could be required to meet a specific

Editor's note—This article is an extended version of the paper [1] that received the "Best Student Paper" award at the 2010 IEEE Wireless and Microwave Technology Conference (WAMICON).

amplifier noise figure target. However, the impact on cascaded system performance might be compromised. Most filter designs are sensitive to mismatch loss, which affects both selectivity and out of band rejection as well as passband response. High port VSWR leads to additional noise figure degradation as well as system distortion. Therefore, a technique which leads to LNA design that achieves low input and output VSWR and low noise measure simultaneously is highly desirable.

The noise figure of a single stage amplifier is a function of the output impedance of the source attached to the input terminals of the transistor. The value of the source impedance which corresponds to a noise figure near the minimum noise figure, $F_{\min}$, is usually different from the source impedance required for conjugate match. Therefore, the input matching network can be tuned for either low VSWR or low noise but not both. Available gain contours and noise contours when plotted on the Smith Chart allow assessment of the trade-off between a good match and low noise figure [3]. In addition, input and output VSWR circles are overlaid allowing the designer to evaluate the mismatch loss. This process is tedious. Noise measure contours, where the noise and gain contours are combined were introduced in [4] to simplify the design process.

One technique for achieving an acceptable tradeoff is by judicious choice of load impedance. Modification of the load impedance alters the input impedance. If properly chosen, the load impedance will permit the source impedance to lie close to the optimum noise impedance. This technique, using an optimization function [5] based on the noise measure, permits a modest improvement in performance. However, noiseless feedback using a reactive component in conjunction with load termination adjustment provides further improvement. Graphical techniques may be used in the process for both adjustments; load termination modification and series feedback [6]. This technique permits the real part of the input impedance to be driven in the direction coincident with the optimum noise impedance through series feedback while simultaneously achieving low input VSWR. These two degrees of freedom assist the designer by permitting the real part of the input impedance to be modified readily. The relationship between the input reflection coefficient of the active two-port and the applied load termination is a bilateral transfer function and is given by equation (2). Reflection feedback for the active device is provided by

$$S'_{11} = S_{11} + \frac{S_{21}S_{12}\Gamma_L}{1 - S_{22}\Gamma_L} \tag{2}$$

whereby the S-parameters of the two-port are modified by the choice of Γ_L, the load reflection coefficient. The reflection feedback in conjunction with the two-port pH-JFET series source feedback leads to a coherent design technique for optimizing the noise figure and the input VSWR at a single frequency. Series source inductive feedback modifies the S-parameters of equation (2). Finding the composite S-parameter set is straightforward by conversion of the active device S-data to Z parameters and adding the matrix sets term for term. The composite set of S-data is subsequently applied in equation (3). Setting the desired input reflection coefficient equal to the optimum noise reflection coefficient yields

$$\Gamma_L(L_s) = \frac{\Gamma^*_{on} - S_{11}(L_s)}{S_{22}(L_s)\Gamma^*_{on} - \Delta(L_s)} \text{ with } |\Gamma_L(L_s)| < 1 \tag{3}$$

where the S-parameters of the active two-port and the determinant of the S-matrix, Δ, are functions of the series feedback inductance, L_s. The optimum noise input reflection coefficient is defined as Γ^*_{on} [7]. We can achieve the desired input conjugate match point and optimum noise match point through the appropriate load reflection coefficient, Γ_L provided by equation (3), if it exists. This may be achieved as L_s goes to zero. However, this is achieved provided the magnitude of the required load reflection is within the boundary of the unit Smith chart. The desired input conjugate match point and optimum noise match point, it if exists, can be achieved through the appropriate Γ_L provided by equation (3). This can be accomplished without the use of series inductive feedback if the condition

$$|S_{22}| > 1 - \frac{S_{12}S_{21}}{\Gamma^*_{on} - S_{11}} \tag{4}$$

is met. If not, then series inductance feedback is required. The constraint of equation (3) is readily met, and the design of the load termination and series feedback is done concurrently to arrive at a suitable $\Gamma_L(L_s)$ using equation (2). Unfortunately, series feedback may lead to instability. Therefore, additional design parameters must be introduced. Multiple amplifier design parameters such as stability factor, noise measure, and return loss may be handled analytically.

However, the insight afforded by analytic techniques is limited and an intuitive understanding of the trade-off between port VSWR, available gain, and the noise figure versus actual feedback inductance versus frequency is not evident. As a result, the design is typically turned over to a CAD tool for optimization. However, it is possible to recast the noise measure equations and the mismatch circles as a function of feedback inductance explicitly. Using

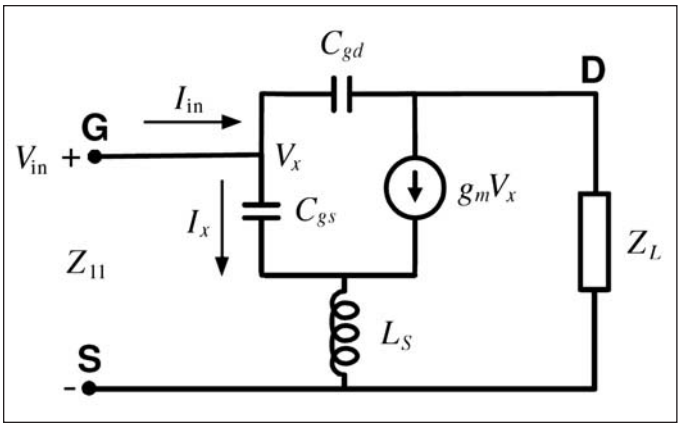

Figure 1 · Simplified pH-JFET input model with series inductive feedback and load termination.

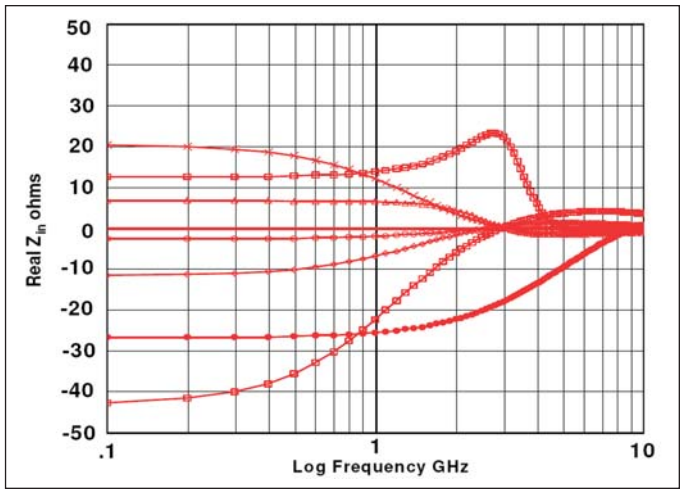

Figure 2 · The real input impedance of Figure 1 is either positive or negative with frequency and is dependent on the active device parameters, the load termination, and the series feedback reactance.

this technique noise measure and mismatch loss as function of feedback inductance are plotted for a specific device. The design curves readily demonstrate whether the feedback is degenerative or regenerative for the chosen device. Furthermore, a new figure-of-merit (FOM) is defined and plotted for the given device that clearly highlights an optimum value for feedback. The minimum value in the plot of figure-of-merit is used to obtain the optimum value of feedback inductance which allows the best trade-off of noise measure, mismatch loss, and avoids instability. A review of the feedback technique and equations for various parameters is presented in the next section and an explanation of possible regeneration is highlighted. In Section III, comparison of simulation results using the new technique with optimized results described in [6] is presented. Finally, in Section IV, experimental results and comparison of measured and simulated data is presented.

II. Circuit Design

A simplified pH-JFET model is shown in Figure 1 and is used for analysis. Mismatch loss is used as a metric to gauge the match between the source impedance and the amplifier port impedance. The loss is derived directly from the two-port transducer gain for a passive network. For this case, $|S_{21}| = |S_{12}| = 1$, $S_{11} = S_{22} = 0$, and the mismatch loss is given by

$$ML = \frac{\left(1-|\Gamma_x|^2\right)\left(1-|\Gamma_y|^2\right)}{\left|1-\Gamma_x\Gamma_y\right|^2} \tag{5}$$

The reflection coefficients, Γ_x and Γ_y provide a measure of the ports relative to the source and the load. In the context of this design work it would be the optimum noise reflection coefficient, either Γ_{on} or Γ_{om} functions of noise measure or noise figure respectively, and the actual input reflection coefficient of the device, Γ_{in}. In this work the emphasis is in applying Γ_{om}.

Stability of the network is assessed by observing the real part of the input impedance, Z_{11}, between the gate source terminals with load termination Z_L. If the gate-drain capacitance is absent or sufficiently small, the series inductance feedback will provide degeneration, while series capacitance provides negative real input impedance. However, adding sufficient gate-drain capacitance and the appropriate load impedance Z_L, will lead to negative real input impedance for the case of series inductance. Figure 2 demonstrates the real part of Z_{11} for a variety of assigned parameters of Figure 1. A broad frequency range of negative input resistance is supported and is both active device and termination dependent. The variations illustrated in Figure 2 are obtained with the load impedance, Z_L and the series feedback always inductive. In addition C_{gs}, C_{gd} and g_m are constrained within a typical range for small low noise FET devices.

Writing an expression for the real part of the input impedance, $\mathrm{Re}(Z_{11})$ with an inductive load impedance Z_L, and feedback C_{gd} present, we get:

$$\mathrm{Re}\left(Z_{11}[\omega, L_s]\right) = \frac{g_m L_s}{C_{gs}+C_{gd}} - \omega^2 \frac{g_m\left(C_{gd}L_s Z_L\right)}{\left(C_{gs}+C_{gd}\right)} + \left(\frac{g_m L_s Z_L}{C_{gs}\left(L_s+Z_L\right)}\right) \tag{6}$$

The imaginary component is part of the input match and is tuned out, while three significant real components remain. The first positive real component leads to degeneration and the ability to alter the input impedance in a

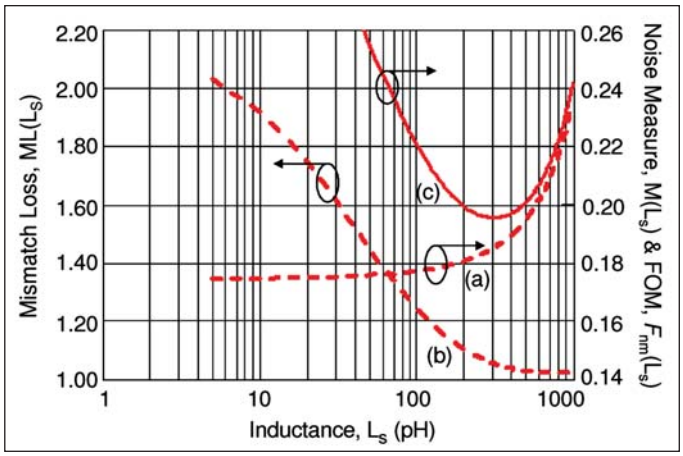

Figure 3 · (a) Noise Measure, M(L_s), (b) Mismatch Loss, $ML(L_s)$, and (c) Figure-of-Merit (FOM), $F_{nm}(L_s)$ for FHX04X as function of L_s. (1)

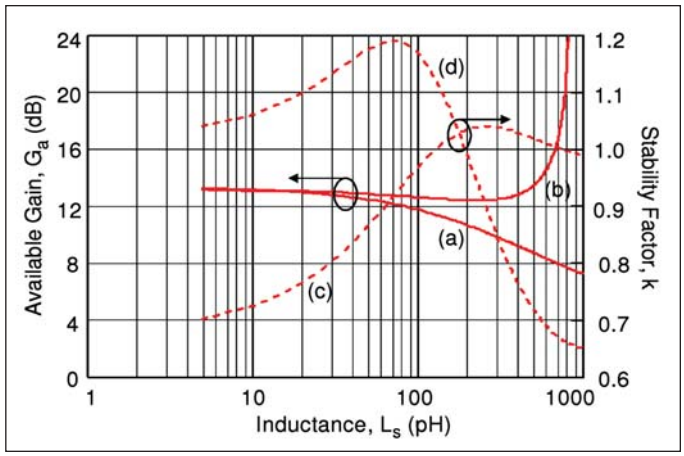

Figure 4 · Available Gain, G_a (solid line) and stability factor, k (dashed line) vs. L_s for FHX040X, (a) and (c) and NE4210S01, (b) and (d). (1)

noiseless manner. A second negative real component leads to regenerative feedback. However, if Z_L is appropriately modified it is possible to achieve conditional stability, assisting in matching the input and the output, and reducing the ports VSWR. The noise measure, $M(L_s)$, and available gain, $G_a(L_s)$, as a function of feedback inductance, L_s can be obtained explicitly. The reflection coefficients, $\Gamma_{om}(L_s)$ and $\Gamma_{in}(L_s)$ are the optimum noise measure and input reflection coefficients respectively with a load termination Γ_L obtained from Z_L. The available gain is calculated with source reflection coefficient set equal to the optimum noise reflection coefficient, $\Gamma_s(L_s) = \Gamma_{om}(L_s)$. Conversion of device S-parameters to Z-parameters allows the addition of the series impedance. The modified S-parameters, $G_a(L_s)$ and $M(L_s)$ are combined for calculation. The expression for M developed in [8] is coupled to conjugate-mismatch-loss ratio or input VSWR to create a new figure-of-merit and design curves inherent to a particular device. Although the minimum value of M is invariant to feedback, M is not. In this application the input VSWR tracks the input impedance presented to the device for minimizing the noise measure, along with the actual input impedance which is a function of the device S-parameters and the load impedance. Using [8] and [9] noise measure $M(L_s)$ is derived as function of the source inductance. The inverse mismatch loss as function of L_s is shown in equation (7) [3]:

$$ML(L_s) = \frac{\left(\left|1-\Gamma_{om}(L_s)\Gamma_{in}(L_s)\right|\right)^2}{\left(1-\left(\left|\Gamma_{om}(L_s)\right|^2\right)\right)\left(1-\left(\left|\Gamma_{in}(L_s)\right|\right)^2\right)} \quad (7)$$

A new figure-of-merit $F_{nm}(L_s)$ is introduced and defined as the product function of noise measure, $M(L_s)$ and mismatch loss, $ML(L_s)$, both functions of L_s.

$$F_{nm}(L_s) = M(L_s) \bullet ML(L_s) \quad (8)$$

For the best trade-off of noise measure and mismatch loss, $F_{nm}(L_s)$ must be minimized. This leads to the optimum value of L_s which can be obtained either graphically or analytically.

III. Comparative Results

The data for the HEMT device FHX04X optimized in [6] was used for comparison with simulation results obtained using the proposed technique. Investigation is conducted at a frequency of 10 GHz.

The trade-off of noise measure and mismatch loss is evident in Figures 3(a) and 3(b). The new figure-of-merit is plotted as a function of source inductance and a minimum occurs for a value of 250 pH; see Figure 3(c). This representation of the benefit of feedback is complementary to that on the Smith chart. In addition, it is easier to interpret than the technique using transducer gain and load admittance plane presented in [10]. Next a set of S-parameters based on a feedback inductance of 250 pH is collected and the matching networks designed and compared to the case where optimization functions are employed, as discussed in [6]. Although the gain is slightly lower at 10.2 dB, the NF is identical and noise measure difference is less than 0.02. The output match is exact and the input VSWR is less than 1.7:1, a 5 dB return loss improvement. Comparative results are highlighted in Table 1.

The available gain as a function of source inductance is plotted in Figure 4(a) for FHX040X and in Figure 4(b) for NE4210S01 (from NEC Corp.). For the latter device the feedback becomes regenerative above 200 pH and gain increases exponentially while available gain contin-

	Noise Measure	VSWR (In)	VSWR (Out)	Gain (dB)
Ref. [4]	0.1634	2.67	2.20	13.4
This work	0.1817	1.66	1.00	10.2

Table 1 · Comparison of simulation data based on Ref. (4) vs. the analytic technique outlined in this work.

ues to decrease monotonically for the former. The stability factor, k, is plotted in Figures 4(c) and 4(d). As seen in 4(d) the feedback is initially degenerative but turns regenerative above 200 pH. Separate calculation of stability factor, k, is not necessary if the new figure-of-merit, F_{nm}, is used for design. This is evident from Figures 3(c) and 5(c), as a significant rise and a steep slope in the function is noted.

IV. Design and Experimental Verification

The low cost pH-JFET, NE4210S01 discussed in the previous section was used in a common source configuration. The S-parameters and noise figure data from the device datasheet at 10.0 GHz and 10.5 GHz were interpolated to obtain the data at 10.24 GHz (see Table 2) and subsequently utilized in a MathCAD® script to create appropriate networks based on theory presented in section III. The input and output terminations were selected after a review of the plots for noise measure and conjugate input mismatch loss, see Figure 5(a) and 5(b). The figure-of-merit for this device is plotted in Figure 5(c). This shows that the optimum value of source inductance is 130 pH, which was chosen for design for best trade-off of noise measure and return loss. If optimum noise match is used, NF is 0.44 dB. While the output match is perfect, the input VSWR under this condition is 2.8. Using the technique outlined in this work, NF is traded off with mismatch loss and is slightly higher at 0.67 dB. The input termination forces an output termination which, if selected, allows a perfect output match. Instead, this output termination is used only to re-calculate a new input reflection coefficient which is subsequently matched. The result is a minimal shift in the noise measure M but a significant drop in input mismatch loss. The output match is sacrificed slightly.

The device was mounted on a 30 mil thick Rogers

S_{11}	S_{12}	S_{21}	S_{22}
0.528/-134	0.096/8.9	4.04/44	0.26/-101
Noise Parameters	Γ_{opt}	R_n	F_{min}
	0.380/101	5.4	0.44

Table 2 · S-parameter (MAG/ANGLE), noise figure, optimum input reflection coefficient and F_{min} in dB at 10.24 GHz.

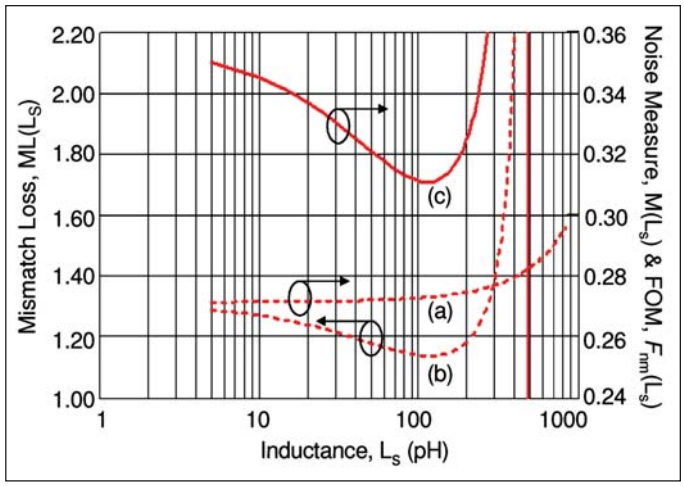

Figure 5 · (a) noise measure, $M(L_s)$, (b) mismatch loss, $ML(L_s)$, and (c) figure-of-merit (FOM) $F_{nm}(L_s)$, for NE4210S01 as function of L_s (1).

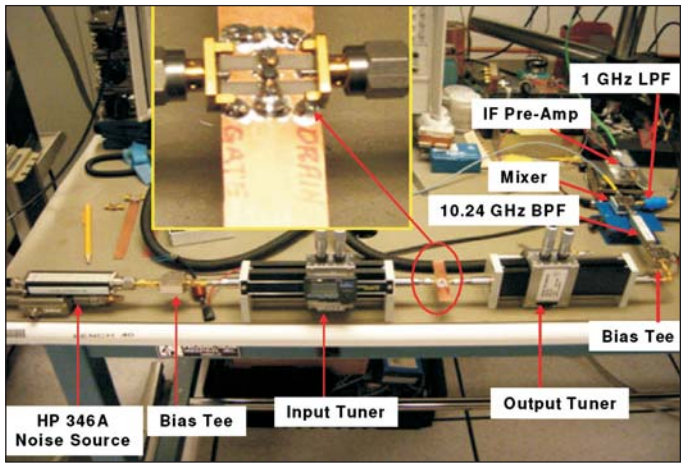

Figure 6 · Test Set up for noise figure and gain measurement at 10.24 GHz (1).

RO4350B laminate and was biased at a V_{dsq} of 2 V and I_{dsq} of 10 mA with a set of bias tees. External tuner matching was used and the device was degenerated by using the package lead inductance and a PCB pad with three additional 40 mil vias.

Measurement device reference plane was located at the lead bend in an SO1 package. Lead extension beyond both source bends added to the desired inductance. The source leads were soldered to a pad and located within 40 mil of the three ground vias. A ground via fence was located both above and below the device. The test setup and a close-up of the device under test (DUT) are shown in Figure. 6.

Measured VSWR shows an excellent input match and an output VSWR less than 1.5:1, see Figure 7. In simulation, the reflection coefficient is held constant over a 160

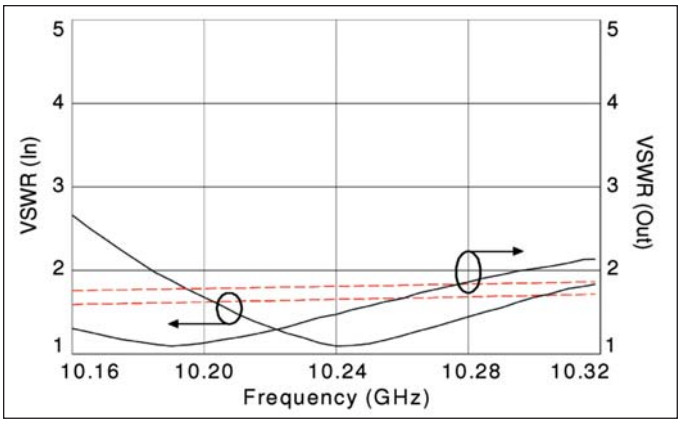

Figure 7 · Comparison of measured (solid) and simulated (dashed) input and output VSWR vs. frequency. The minimum value occurs at a source inductance of approximately 130 pH. In simulation, the reflection coefficient is held constant. (1).

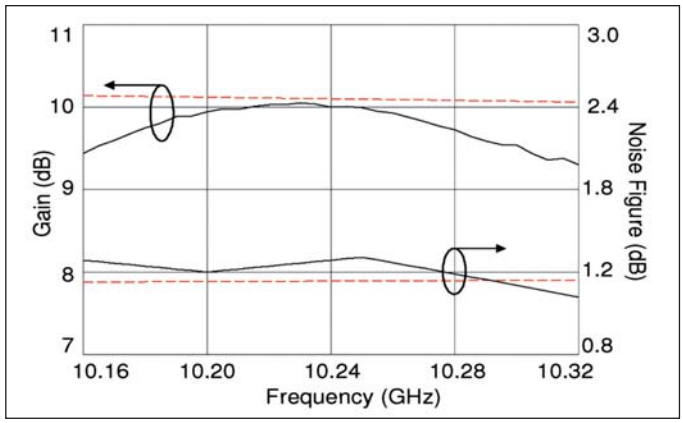

Figure 8 · Comparison of measured (solid) and simulated (dash) available gain and noise figure vs. frequency. In simulation, the reflection coefficient is held constant. (1)

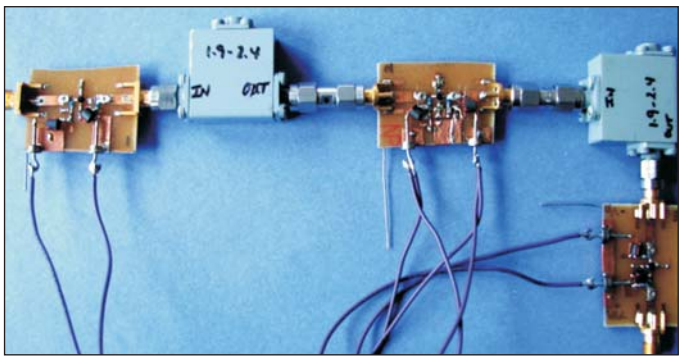

Figure 9 · Three stage cascaded amplifier with series degenerative feedback in each stage.

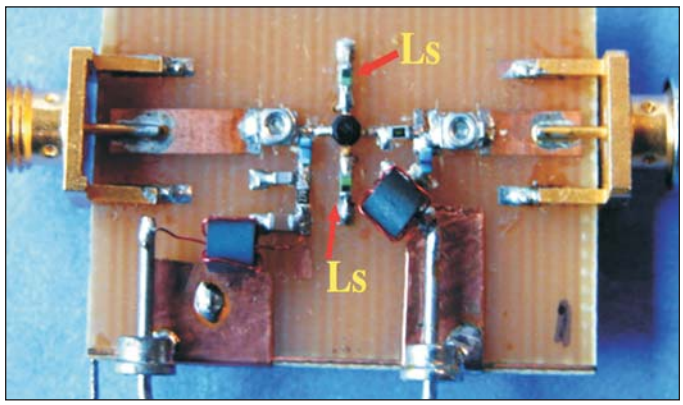

Figure 10 · Close-up of one of three amplifiers incorporating series feedback. The 3-stage cascade provides 46 dB of available gain at 2.1 GHz with 0.54 dB noise figure.

MHz bandwidth around a center frequency of 10.24 GHz and does not emulate the tuner response over the measured band. Simulation shows a NF of 1.37 dB across the bandwidth of interest when corrected for 0.7 dB fixture loss. Noise figure (NF) measurement was single sideband (SSB) using a down conversion mixer-filter centered at 10.24 GHz. Bias tee, tuner loss, and second stage contribution loss were accounted for in NF measurement. Although input reflection coefficient is held constant in simulations, measured NF shows good agreement, see Figure 8. Gain measurement does not account for tuner and bias loss of 3.2 dB. Simulation therefore is offset by this loss for purpose of comparison. The insertion gain is 10 dB and is in good agreement with simulation at the center frequency, see Figure 8. Stability was monitored using a directional coupler and spectrum analyzer at 10.24 GHz. Adjustment of the amplifier for best input return loss at band center resulted in the lowest noise figure. Any readjustment of the input tuner degraded the noise figure measurement.

The technique discussed was also applied to cascaded amplifier stages at 2.1 GHz, see Figure 9. Discrete inductive feedback was added to each of the FET sources as shown in detail in Figure 10. Isolators applied at interstage locations were added to facilitate noise figure measurement of the cascade using an extended manual *Y*-factor measurement method [11]. Minimization of the merit function lead to individual noise figures of less than 0.5 dB. Although the input return loss was excellent, better than 20 dB return loss, the output return loss was less than 10 dB. The output return loss was subsequently improved and the input return loss degraded while still maintaining an optimum input noise termination. Each port return loss was set to 15 dB and a cascade of three stages was readily completed. The final cascade gain is 46 dB while providing a noise figure total of 0.54

dB which included second and third stage noise figure contributions.

Summary and Conclusions

A new analytic technique and a figure-of-merit for optimizing the feedback inductance for degeneration in a low noise amplifier were discussed. The plot of noise measure and mismatch loss together serve as a valuable guide in optimizing the design and avoiding instability. The plot of the figure-of-merit enables the selection of optimum inductance. The well established approach to noise matching, working from the input side of the amplifier to the output can potentially be improved. As a proof-of-concept an X-band LNA was designed and measured. The output termination was chosen first based on the optimum noise measure and input reflection coefficient and the information from the design curves as a function of feedback inductance. The output match degrades slightly but the input match is perfect. The noise measure increases minimally, demonstrating the desired trade-off.

References

1. A. Victor, and J. Nath, "Simultaneous Input Power Match and Noise Optimization Using Feedback," *Proc. IEEE Wireless & Microw. Tech. Conf.*, Apr. 2010.

2. H. A. Haus, and R. B. Adler, "Optimum Noise Performance of Linear Amplifier," *Proc. IRE*, Aug. 1958, pp. 1517-1533.

3. G. Gonzalez, *Microwave Transistor Amplifiers Analysis and Design*, Prentice Hall, 1997.

4. H. Fukui, "Available power Gain, Noise figure, and Noise Measure of Two-Ports and Their Graphical Representations," *IEEE Trans. Cir. Theory*, vol. 13, no. 2, Jun.1966, pp. 137-142.

5. K. W. Eccleston, "Port-Match Optimization of Microwave Low-Noise Amplifiers," *Microw. Opti. Techn. Lett.*, vol. 27, no. 5, Dec. 2000, pp. 321-323.

6. R. E. Lehmann and D. D. Heston, "X-Band Monolithic series feedback LNA," *IEEE Tran. Microw. Theory Techn.*, vol. 33, no. 12, Dec. 1985, pp. 1560-1566.

7. Masataka Mitama, Hidehiko Katoh, "An Improved Computational Method for Noise Parameter Measurement," *IEEE Trans. Microw. Theory Techn.*, vol. 27, pp. 612-615, June 1979.

8. C. R. Poole, and D. K. Paul, "Optimum Noise Measure Terminations for Microwave Transistor Amplifiers," *IEEE Tran. Microw. Theory Techn.*, vol. 33, no. 11, Nov. 1985, pp. 1254-1257.

9. H. Javan, "Noise Measure for Optimum Broadband Design," *IEE Proc. Cir. Dev. Sys.*, vol. 138, no. 1, Feb. 1991, pp. 1-4.

10. J. Engberg, "Simultaneous Input Power Match and Noise Optimization Using Feedback," in *Proc. Eur. Microw. Conf.*, Oct 1974, pp 385-389

11. A.M. Victor, and M.B. Steer, "Improved Y factor measurement using the second stage contribution to advantage," *IEEE 65th ARFTG Conference Digest*, Spring 2005.

Author Information

Alan Victor is currently a Principal RF Engineer at Nitronex Corporation. He received the BSEE degree from the University of Florida, the MSE degree from Florida Atlantic University and recently received a PhD from North Carolina State University. Dr. Victor has several international patents in communications circuits and his main interests are in low noise circuits, power oscillators, and the application of ferroelectric materials. He can be reached at: amvictor@ncsu.edu

Jayesh Nath received the BE degree (with honors) in electronics and communication engineering from the Birla Institute of Technology, India, and the PhD degree in electrical engineering (with a minor in materials science and engineering) from North Carolina State University. Presently, he is with Aviat Networks where he is involved with product design and development in field of RF/microwave communication. His main research interests include the design, characterization, and modeling RF and microwave devices and systems, electromagnetic design and modeling, measurement and calibration techniques, integrated passives, and 3-D packaging.